Composites: Part B 73 (2015) 72–81

Contents lists available at ScienceDirect

Composites: Part B

journal homepage: www.elsevier.com/locate/compositesb

Vibration analysis of two orthogonal slender single-walled carbon nanotubes with a new insight into continuum-based modeling of van der Waals forces

Keivan Kiani *

Department of Civil Engineering, K.N. Toosi University of Technology, Valiasr Ave., P.O. Box 15875-4416, Tehran, Iran

ARTICLE INFO

Article history:
Received 23 September 2014
Received in revised form 11 December 2014
Accepted 15 December 2014
Available online 24 December 2014

Keywords:
A. Nano-structures
B. Vibration
C. Computational modeling
Doubly orthogonal single-walled carbon nanotubes

ABSTRACT

Transverse vibrations of doubly orthogonal slender single-walled carbon nanotubes (SWCNTs) at the vicinity of each other are of interest. The van der Waals (vdW) forces play an important role in dynamic interactions between two adjacent nanotubes. Using Lennard-Jones potential function, such a phenomenon is appropriately modeled by a newly introduced vdW force density function. By employing Hamilton's principle, the equations of motion are obtained based on the nonlocal Rayleigh beam theory. In fact, these are integro-partial differential equations and seeking an exact or even analytical solution to them is a very difficult job. Therefore, an efficient numerical solution is proposed. The effects of the inter-tube distance, slenderness ratio, small-scale parameter, aspect ratio, and elastic properties of the surrounding medium on the free vibration of the nanosystem are addressed. The obtained results could be regarded as a pivotal step for better realizing of dynamic behaviors of more complex systems consist of multiple orthogonal networks of nanotubes.

1. Introduction

Since the past decade, vibrations of carbon nanotubes (CNTs) have been of focus of attention of the communities of material, structural, and mechanical engineering [1–9]. It is mainly related to the excellent physical, chemical, and mechanical properties of such newly synthesized materials [10–14] in which provide them for a wide range of applications including sensors (both physical and chemical) [15–17], resonators [18–20], nanofluids conveyors [21–23], drug delivery [24–27], and micro-/nano- electromechanical systems (MEMS/NEMS) [28–31]. In all above-mentioned applications, understanding the true mechanics of dynamical behavior of CNTs will surely lead to a more efficient and optimal nanosystem.

To date, vibrations of single-walled carbon nanotubes (SWCNTs) has been broadly examined including free dynamic response [32–34], excitations due to a moving nanoparticle [35–37], wave propagation [38–42], vibrations due to inside fluids flow [43–46], and nonlinear free and forced vibrations [47–49]. Additionally, transverse vibrations of a system of doubly parallel nanobeams were investigated [50,51]. In the latter two works, the interactional van der Waals (vdW) forces between atoms of the adjacent nanostructures were simply modeled by a continuous transverse spring without careful evaluating the spring's constant. In a more general framework, vibrations of two- and three-dimensional ensembles of SWCNTs were also carefully addressed [52–54]. In all these studies, the straight individual tubes were placed parallel to each other and at equal distances from each other. The interactions of adjacent tubes were modeled by appropriate springs whose constants were methodically calculated. A brief review of all above-mentioned works reveals that the vdW forces between neighboring tubes have been modeled by elastic layers whose properties were constant and uniform across the tubes' lengths. The unit of the spring constants is $\frac{N}{m^2}$. It means that the interactional vdW forces between two neighboring tubes was considered as a product of the spring constant and the difference of their transverse displacements. In an attempt for factual modeling of such forces, the vibration problem of a system of double-orthogonal-SWCNTs (DOSWCNTs) is visited in this paper. The obtained results will display that the vdW forces between two tubes are incorporated into the model by a so-called vdW force density function of unit $\frac{N}{m^3}$. In contrast to the previous works, the present work suggests that a more pragmatic version of the vdW force between two adjacent tubes is an integral of the product of the vdW force density function and the difference of transverse

* Tel.: +98 21 88779473; fax: +98 21 88779476.
E-mail addresses: k_kiani@kntu.ac.ir, keivankiani@yahoo.com

http://dx.doi.org/10.1016/j.compositesb.2014.12.025
1359-8368/

displacements over the tube's length. Due to this fact, the resulting equations of motion are coupled integro-partial differential equations. It is expected that such a newly established model would lead to a more accurate prediction of free vibrations of DOSWCNTs as well as other systems composed of SWCNTs.

The classical continuum theory (CCT) cannot capture the realistic vibrations of nanostructures since the inter-atomic bonds are not introduced to the constitutive relations [55–57]. When the ratio of the bond's length to the nanostructure's length or wavelength of the propagated wave becomes comparable, the effect of the inter-atomic bonds becomes significant (i.e., size-dependency). In such cases, the stress state of each point does not only depend on the stress of that point, but also to the stress states of its neighboring points (i.e., nonlocality). To conquer such a shortage of the CCT, several advanced continuum theories (ACTs) have been established. One of the most well-known theories is the nonlocal continuum field theory of Eringen [68–71]. So far, such a theory has been extensively employed in mechanical modeling of CNTs [37–41,43,46,49,52–54,58,59]. Another popular ACT is the strain gradient theory of Aifantis [60,61] which is also implemented in modeling vibrations of CNTs [62–67].

Since flexural behavior of slender DOSWCNTs is of interest, a nonlocal model based on the Rayleigh beam theory is developed. In such nanosystems, the share of shear strain energy in the total strain energy can be rationally ignored since the ratio of shear strain energy to the flexural strain energy is fairly negligible. For dynamic analysis of stocky CNTs, application of shear deformable beam models would lead to more accurate results [49,53,54,63].

In the present work, using Lennard-Jones potential function, the vdW force density function is introduced. By employing nonlocal Rayleigh beam theory, nonlocal-integro-partial differential equations describe transverse vibrations of the nanosystem are obtained. Seeking an analytical solution to these coupled equations is a very difficult task. By using Galerkin approach in conjunction with assumed mode method, the deflection fields of the nanotubes are discretized in the dimensionless spatial domains of tubes. Subsequently, the natural frequencies of the nanosystem are numerically determined. Through various parametric studies, the influences of the slenderness ratio, intertube distance, aspect ratio, size-dependency, transverse and rotational stiffness of the surrounding elastic medium on the free vibration behavior are studied. The undertaken work can be taken into account as a primary step for better realizing of more complex structures composed of orthogonal membranes of SWCNTs or even multi-walled carbon nanotubes.

2. Assessment of vdW forces between two orthogonal SWCNTs

Based on the Lennard-Jones potential function [72], the interaction between two neutral atoms at distance λ is given by:

$$\Phi(\lambda)=4\epsilon\left[\left(\frac{\sigma}{\lambda}\right)^{12}-\left(\frac{\sigma}{\lambda}\right)^{6}\right], \tag{1}$$

where ϵ is the depth of the potential well, σ denotes the distance at which the potential function becomes zero and is expressed by: $\sigma=\frac{r_a}{\sqrt[6]{2}}$ where r_a is the distance between two atoms at the equilibrium state (i.e., the inter-particle potential reaches its absolute minimum value). The vdW force between a pair of atoms i and j, $\mathbf{f}_{ij}$, is formulated as follows:

$$\mathbf{f}_{ij}=-\frac{\mathrm{d}\Phi}{\mathrm{d}\lambda}\mathbf{e}_{\lambda}=\frac{24\epsilon}{\sigma^2}\left[2\left(\frac{\sigma}{\lambda}\right)^{14}-\left(\frac{\sigma}{\lambda}\right)^{8}\right]\vec{\lambda}, \tag{2}$$

where $\vec{\lambda}$ is the vector position of the atom j with respect to the atom i, and $\mathbf{e}_{\lambda}$ denotes the corresponding unit base vector. According to the Cartesian and cylindrical coordinate systems pertinent to the orthogonal nanotubes (see Fig. 1(a) and (b)), the walls' geometry of these transversely deformed tubes is described by: $(x_1,y_1=r_{m_1}\cos\phi_1,z_1=r_{m_1}\sin\phi_1+w_1(x_1,t))$ and $(x_2,y_2=r_{m_2}\cos\phi_2,z_2=r_{m_2}\sin\phi_2+w_2(x_2,t))$ where d is the intertube distance, $0\leqslant x_i\leqslant l_{b_i}$ and $0\leqslant\varphi_i\leqslant 2\pi$; $i=1,2$. On the basis of the Cartesian coordinate system associated with the first nanotube,

$$\begin{aligned}\vec{\lambda}=&(x_1-l_{11}-r_{m_2}\cos\varphi_2)\mathbf{e}_{x_1}+(r_{m_1}\cos\varphi_1-x_2+l_{21})\mathbf{e}_{y_1}\\&+(r_{m_1}\sin\varphi_1-r_{m_2}\sin\varphi_2+d-\triangle w)\mathbf{e}_{z_1},\end{aligned} \tag{3}$$

where $\mathbf{e}_{x_1}$, $\mathbf{e}_{y_1}$, and $\mathbf{e}_{z_1}$ are the unit base vectors associated with the rectangular coordinate system of the nanotube 1, r_{m_i} is the mean radius of the equivalent continuum structure pertinent to the ith tube, $\triangle w=w_2(x_2,t)-w_1(x_1,t)$, and $w_i(x_i,t)$ represents the transverse displacement field of the ith SWCNT along the z_1 axis. The interactional vdW force per unit square length of tubes due to their relative transverse motions along the z_1 axis is described by:

$$f_z=\frac{24\epsilon\sigma_{CNT}^2}{\sigma^2}\int_0^{2\pi}\int_0^{2\pi}\left[2\left(\frac{\sigma}{\lambda}\right)^{14}-\left(\frac{\sigma}{\lambda}\right)^{8}\right]\begin{pmatrix}r_{m_1}\sin\varphi_1-r_{m_2}\sin\varphi_2+\\ d-\triangle w\end{pmatrix}\mathrm{d}\varphi_1\,\mathrm{d}\varphi_2, \tag{4}$$

where $f_z=f_z(x_1,x_2,t)$, $\sigma_{CNT}=\frac{4\sqrt{3}}{9a^2}$ denotes the surface density of the carbon atoms, and a is the length of the carbon–carbon bond. In order to evaluate the change in vdW force per unit square length due to the small lateral displacements of the nanotubes, it is only suffice to approximate Eq. (4) by the Taylor expansion up to the first-order about the equilibrium state. By doing so, the extra transverse vdW force per unit square length is calculated as:

$$\triangle f_z=C_{vdW}(x_1,x_2)\triangle w, \tag{5}$$

where

$$\begin{aligned}C_{vdW}(x_1,x_2;r_{m_1},r_{m_2},d)=&-\frac{256\epsilon r_{m_1}r_{m_2}}{9a^4}\\&\times\int_0^{2\pi}\int_0^{2\pi}\left\{\begin{matrix}\sigma^{12}\left[\varrho^{-7}-14\varrho^{-8}\left(d+r_{m_1}\sin\varphi_1-r_{m_2}\sin\varphi_2\right)^2\right]\\ -\frac{\sigma^6}{2}\left[\varrho^{-4}-8\varrho^{-5}\left(d+r_{m_1}\sin\varphi_1-r_{m_2}\sin\varphi_2\right)^2\right]\end{matrix}\right\}\mathrm{d}\varphi_1\,\mathrm{d}\varphi_2,\end{aligned} \tag{6a}$$

$$\begin{aligned}\varrho(x_1,x_2,\varphi_1,\varphi_2;r_{m_1},r_{m_2},d)=&\left(x_1-l_{11}-r_{m_2}\cos\varphi_2\right)^2\\&+\left(x_2-l_{21}-r_{m_1}\cos\varphi_1\right)^2+\left(r_{m_1}\sin\varphi_1-r_{m_2}\sin\varphi_2+d\right)^2.\end{aligned} \tag{6b}$$

The parameter C_{vdW} is called the vdW force density function (since its unit is $\frac{\mathrm{N}}{\mathrm{m}^3}$). As it is seen in Eq. (6), radii of the nanotubes, the intertube distance, and the location of the nanotubes' intersection are among the crucial factors that influence on this parameter.

To see the variation of C_{vdW} in the spatial coordinates associated with the nanotubes, let give an example. Consider a system of DOSWCNTs whose tubes cross each other at the midspan point. The geometry of the nanosystem is as: $l_{b_1}=l_{b_2}=30$ nm, $r_{m_1}=r_{m_2}=1.5$ nm, $d=r_{m_1}+r_{m_2}+2t_b$, and $l_{11}=l_{21}=\frac{l_{b_1}}{2}$. In order to evaluate the double integral in Eq. (6a), Gauss quadrature method is exploited. The pyramid of each tube is divided into 10 equal subdomains with 5 Gauss points. The graph of C_{vdW} in terms of dimensionless spatial coordinates of tubes, namely $\xi_1=\frac{x_1}{l_{b_1}}$ and $\xi_2=\frac{x_2}{l_{b_1}}$, has been demonstrated in Fig. 2. As it is seen, shooting of the vdW force density function at the midspan point of both tubes is so obvious. Further studies also reveal that such a fact occurs at the vicinity of the intersection point of the tubes. As a result, a more refined mesh should be considered for evaluating integrals of expressions include C_{vdW} in the regions close to the point of intersection (see Fig. 2). In all carried out calculations in this paper, we subdivide the lengths of tubes into N_p-1 intervals such that about half of them are equally located in a region of length $0.1l_{b_1}$ or $0.1l_{b_2}$ around the intersection point. By choosing N_g Gaussian point in each direction (or $N_g\times N_g$ in each computational cell), a

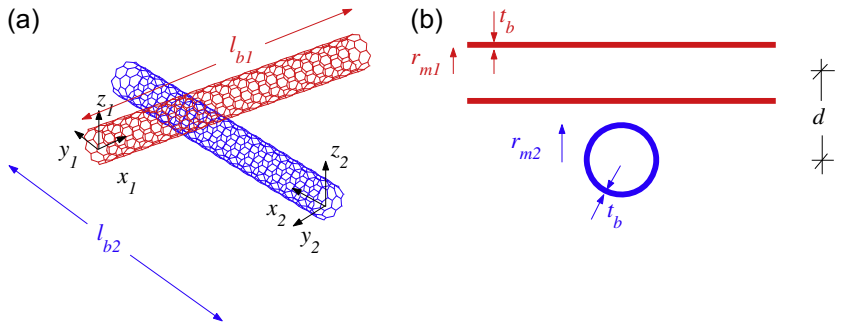

Fig. 1. (a) A system of doubly orthogonal SWCNTs at the vicinity of each other. (b) Equivalent continuum-based nanostructures.

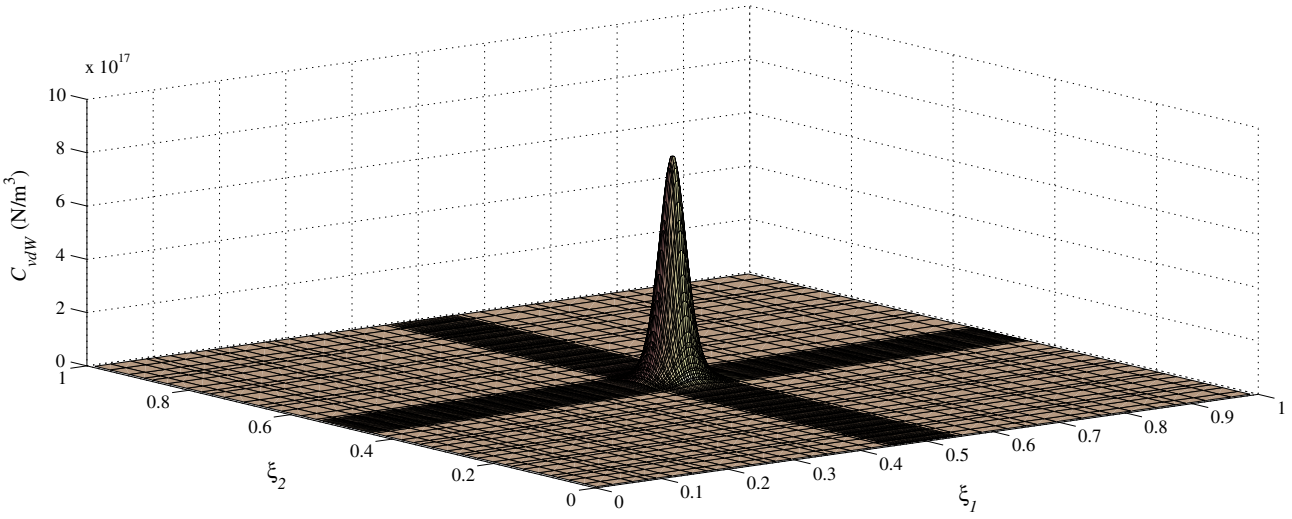

Fig. 2. Plot of the vdW force density function for a system of DOSWCNTs.

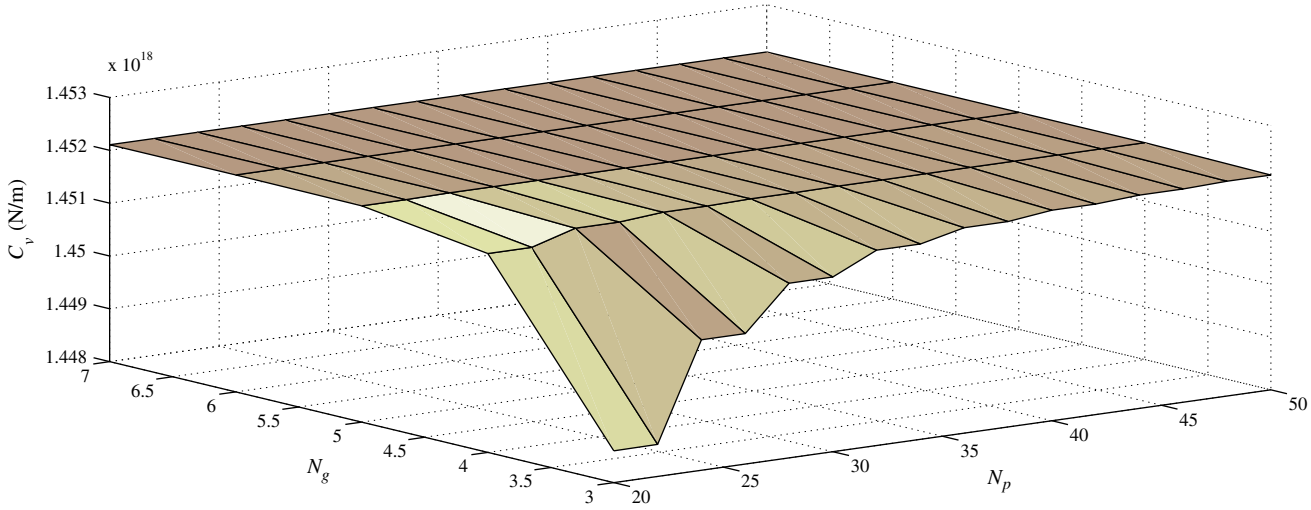

Fig. 3. Convergence check of the numerically evaluated $C_v = \int_0^1 \int_0^\gamma C_{vdW} d\xi_1 d\xi_2$ as a function of the number of Gaussian points (N_g) and the number of grids (N_p) in each direction.

convergence check is performed. Suppose that evaluation of $C_v = \int_0^1 \int_0^1 C_{vdW}(\xi_1, \xi_2) d\xi_1 d\xi_2$ is of concern. By following up the above-mentioned strategy, the predicted results of C_v as a function of N_p and N_g have been demonstrated in Fig. 3. This figure displays that by an increase of Gaussian points as well as subdivisions, the computed value of C_v would converge to a specific value. Based on this investigation, we use 30×30 computational cells with 4×4 Gaussian points in each cell for evaluation of double integrals associated with C_{vdW}.

The linear elastic energy resulted from the given vdW force density function for a system of doubly orthogonal SWCNTs is calculated as:

$$U_{vdW}(t)=\frac{1}{2}\int_{x_1=0}^{l_{b_1}}\int_{x_2=0}^{l_{b_2}}C_{vdW}(x_1,x_2)(w_1(x_1,t)-w_2(x_2,t))^2\,\mathrm{d}x_1\mathrm{d}x_2. \tag{7}$$

In the upcoming part, Eq. (7) is exploited to construct equations of motion of a double-orthogonal SWCNTs-system by employing Hamilton's principle.

3. Free vibration analysis of DOSWCNTs

3.1. Nonlocal governing equations

At each time t, the kinetic energy (T) and the nonlocal elastic strain energy of a system of elastically embedded DOSWCNTs (U) based on the Rayleigh beam theory are expressed by:

$$T(t)=\frac{1}{2}\int_0^{l_{b_1}}\rho_{b_1}\left(A_{b_1}\left(\frac{\partial w_1(x_1,t)}{\partial t}\right)^2+I_{b_1}\left(\frac{\partial^2 w_1(x_1,t)}{\partial t\partial x_1}\right)^2\right)\mathrm{d}x_1 +\frac{1}{2}\int_0^{l_{b_2}}\rho_{b_2}\left(A_{b_2}\left(\frac{\partial w_2(x_2,t)}{\partial t}\right)^2+I_{b_2}\left(\frac{\partial^2 w_2(x_2,t)}{\partial t\partial x_2}\right)^2\right)\mathrm{d}x_2, \tag{8a}$$

$$U(t)=\frac{1}{2}\int_{x_1=0}^{l_{b_1}}\left(-\frac{\partial^2 w_1(x_1,t)}{\partial x_1^2}M_{b_1}^{nl}(x_1,t)+K_t(w_1(x_1,t))^2+K_r\left(\frac{\partial w_1(x_1,t)}{\partial x_1}\right)^2\right)\mathrm{d}x_1 +\frac{1}{2}\int_{x_2=0}^{l_{b_2}}\left(-\frac{\partial^2 w_2(x_2,t)}{\partial x_2^2}M_{b_2}^{nl}(x_2,t)+K_t(w_2(x_2,t))^2+K_r\left(\frac{\partial w_2(x_2,t)}{\partial x_2}\right)^2\right)\mathrm{d}x_2 +\frac{1}{2}\int_{x_1=0}^{l_{b_1}}\int_{x_2=0}^{l_{b_2}}C_{vdW}(x_1,x_2)(w_2(x_2,t)-w_1(x_1,t))^2\,\mathrm{d}x_1\mathrm{d}x_2, \tag{8b}$$

where ∂ is the partial symbol, A_{b_i} and I_{b_i} in order are the cross-sectional area and its moment inertia of the ith tube, w_i and $M_{b_i}^{nl}(x_i,t)$ in order represent the deflection and nonlocal bending moment field associated with the ith SWCNT, K_t and K_r denote the constants of the transverse and rotational continuous springs, respectively. Based on the elastic properties of the surrounding medium of the nanosystem, such constants can be readily determined. In a more realistic model, the continuum of the elastic matrix as well as the existing atomic-bonds between the neighboring atoms of the matrix and those of the DOSWCNTs should be taken into account. However, herein, we mainly focus on the dynamic interactions between the orthogonal nanotubes and their interactions with the surrounding elastic media are simply modeled by elastic layers with the above-mentioned properties.

The nonlocal bending moments within the SWCNTs are related to their local counterparts by [38,73,74]:

$$M_{b_1}^{nl}-(e_0a)_1^2\frac{\partial^2 M_{b_1}^{nl}}{\partial x_1^2}=-E_{b_1}I_{b_1}\frac{\partial^2 w_1}{\partial x_1^2}, \tag{9a}$$

$$M_{b_2}^{nl}-(e_0a)_2^2\frac{\partial^2 M_{b_2}^{nl}}{\partial x_2^2}=-E_{b_2}I_{b_2}\frac{\partial^2 w_2}{\partial x_2^2}, \tag{9b}$$

where E_{b_i}, and $(e_0a)_i$ in order are the Young's modulus, and the small-scale parameter associated with the ith continuum tube. The work of Duan et al. [75] revealed that the aspect ratio, chirality, and boundary conditions of a SWCNT are among the crucial parameters that affect on the small-scale parameter. Thereby, the values of this parameter for the constitutive nanotubes of the DOSWCNTs have been considered to be dissimilar. Generally, the magnitude of this parameter is determined on the basis of the best fit between the predicted dispersion curve by the nonlocal model and that of an appropriate atomic model.

By employing Hamilton's principle, $\int_{t_1}^{t_2}(T(t)-U(t))\,\mathrm{d}t=0$, the nonlocal equations of motion of a system of elastically embedded DOSWCNTs in terms of the nonlocal forces within the tubes are obtained as follows:

$$\rho_{b_1}\left(A_{b_1}\frac{\partial^2 w_1}{\partial t^2}-I_{b_1}\frac{\partial^4 w_1}{\partial t^2\partial x_1^2}\right)-\frac{\partial^2 M_{b_1}^{nl}}{\partial x_1^2}+\int_{x_2=0}^{l_{b_2}}C_{vdW}(w_1-w_2)\,\mathrm{d}x_2 +K_tw_1-K_r\frac{\partial^2 w_1}{\partial x_1^2}=0, \tag{10a}$$

$$\rho_{b_2}\left(A_{b_2}\frac{\partial^2 w_2}{\partial t^2}-I_{b_2}\frac{\partial^4 w_2}{\partial t^2\partial x_2^2}\right)-\frac{\partial^2 M_{b_2}^{nl}}{\partial x_2^2}-\int_{x_1=0}^{l_{b_1}}C_{vdW}(w_1-w_2)\,\mathrm{d}x_1 +K_tw_2-K_r\frac{\partial^2 w_2}{\partial x_2^2}=0. \tag{10b}$$

By introducing Eqs. (9a) and (9b) to Eqs. (10a) and (10b) through assuming the following relations:

$$\frac{\partial^2}{\partial x_1^2}\left[\int_{x_2=0}^{l_{b_2}}C_{vdW}(w_1-w_2)\,\mathrm{d}x_2\right]\approx\int_{x_2=0}^{l_{b_2}}C_{vdW}\frac{\partial^2 w_1}{\partial x_1^2}\,\mathrm{d}x_2, \tag{11a}$$

$$\frac{\partial^2}{\partial x_2^2}\left[\int_{x_1=0}^{l_{b_1}}C_{vdW}(w_1-w_2)\,\mathrm{d}x_1\right]\approx-\int_{x_1=0}^{l_{b_1}}C_{vdW}\frac{\partial^2 w_2}{\partial x_2^2}\,\mathrm{d}x_1, \tag{11b}$$

the nonlocal governing equations of the nanosystem in terms of the deformation fields are obtained as:

$$\rho_{b_1}A_{b_1}\left(\frac{\partial^2 w_1}{\partial t^2}-(e_0a)_1^2\frac{\partial^2 w_1}{\partial t^2\partial x_1^2}\right)-\rho_{b_1}I_{b_1}\left(\frac{\partial^4 w_1}{\partial t^2\partial x_1^2}-(e_0a)_1^2\frac{\partial^6 w_1}{\partial t^2\partial x_1^4}\right) +\int_{x_1=0}^{l_{b_2}}C_{vdW}\left(w_1-w_2-(e_0a)_1^2\frac{\partial^2 w_1}{\partial x_1^2}\right)\mathrm{d}x_2+E_{b_1}I_{b_1}\frac{\partial^4 w_1}{\partial x_1^4} +K_t\left(w_1-(e_0a)_1^2\frac{\partial^2 w_1}{\partial x_1^2}\right)-K_r\left(\frac{\partial^2 w_1}{\partial x_1^2}-(e_0a)_1^2\frac{\partial^4 w_1}{\partial x_1^4}\right)=0, \tag{12a}$$

$$\rho_{b_2}A_{b_2}\left(\frac{\partial^2 w_2}{\partial t^2}-(e_0a)_2^2\frac{\partial^2 w_2}{\partial t^2\partial x_2^2}\right)-\rho_{b_2}I_{b_2}\left(\frac{\partial^4 w_2}{\partial t^2\partial x_2^2}-(e_0a)_2^2\frac{\partial^6 w_2}{\partial t^2\partial x_2^4}\right) +\int_{x_1=0}^{l_{b_1}}C_{vdW}\left(w_2-w_1-(e_0a)_2^2\frac{\partial^2 w_2}{\partial x_2^2}\right)\mathrm{d}x_1+E_{b_2}I_{b_2}\frac{\partial^4 w_2}{\partial x_2^4} +K_t\left(w_2-(e_0a)_2^2\frac{\partial^2 w_2}{\partial x_2^2}\right)-K_r\left(\frac{\partial^2 w_2}{\partial x_2^2}-(e_0a)_2^2\frac{\partial^4 w_2}{\partial x_2^4}\right)=0. \tag{12b}$$

Eqs. (12a) and (12b) furnish us regarding free transverse vibrations of a double-orthogonal nanotube-system which is elastically restrained by a matrix. It is emphasized that these equations are valid for two separate orthogonal SWCNTs at the vicinity of each other. In the case of doubly connected nanotubes at a point, special treatments should be taken into account in modeling of the problem. For example, if transverse vibrations of such a nanosystem is of concern, the most important condition that should be met is the equality of the deflection fields of the nanotubes at the intersection point during the course of contact. Under certain conditions, the nanosystem may sequentially switch between the in-contact and not-in-contact states. In another illustration, if both longitudinal and transverse vibrations of the nanotubes are of interest, one also confronts the sliding problem of the nanotubes and the dynamical contact forces could play a crucial role in vibrations of the nanosystem. To date, the answers to these important issues have not been replied by the scientific communities. These fascinating problems could be considered as hot topics for future works.

In order to study the problem in a more general framework, the following dimensionless quantities are considered:

$$\xi_i=\frac{x_i}{l_{b_1}},\ \tau=\frac{1}{l_{b_1}^2}\sqrt{\frac{E_{b_1}I_{b_1}}{\rho_{b_1}A_{b_1}}}t,\ \mu_i=\frac{(e_0a)_i}{l_{b_1}},\ \lambda_1=\frac{l_{b_1}}{r_{b_1}},\ \overline{w}_i=\frac{w_i}{l_{b_1}};\ i=1,2, \tag{13}$$

by introducing Eq. (13) to Eqs. (12a) and (12b), the dimensionless-nonlocal equations of motion of elastically embedded DOSWCNTs are derived as:

$$\frac{\partial^2\overline{w}_1}{\partial\tau^2}-\mu_1^2\frac{\partial^4\overline{w}_1}{\partial\tau^2\partial\xi_1^2}-\lambda_1^{-2}\left(\frac{\partial^4\overline{w}_1}{\partial\tau^2\partial\xi_1^2}-\mu_1^2\frac{\partial^6\overline{w}_1}{\partial\tau^2\partial\xi_1^4}\right)+\frac{\partial^4\overline{w}_1}{\partial\xi_1^4}$$
$$+\underline{\underline{\int_{\xi_2=0}^{\chi}\overline{C}_{vdW}\left(\overline{w}_1-\overline{w}_2-\mu_1^2\frac{\partial^2\overline{w}_1}{\partial\xi_1^2}\right)\mathrm{d}\xi_2}}+\overline{K}_t\left(\overline{w}_1-\mu_1^2\frac{\partial^2\overline{w}_1}{\partial\xi_1^2}\right)$$
$$-\overline{K}_r\left(\frac{\partial^2\overline{w}_1}{\partial\xi_1^2}-\mu_1^2\frac{\partial^4\overline{w}_1}{\partial\xi_1^4}\right)=0, \tag{14a}$$

$$\varrho_1^2\left(\frac{\partial^2\overline{w}_2}{\partial\tau^2}-\mu_2^2\frac{\partial^4\overline{w}_2}{\partial\tau^2\partial\xi_2^2}\right)-\varrho_2^2\lambda_1^{-2}\left(\frac{\partial^4\overline{w}_2}{\partial\tau^2\partial\xi_2^2}-\mu_2^2\frac{\partial^6\overline{w}_2}{\partial\tau^2\partial\xi_2^4}\right)$$
$$+\varrho_3^2\frac{\partial^4\overline{w}_2}{\partial\xi^4}+\underline{\underline{\int_{\xi_1=0}^{1}\overline{C}_{vdW}\left(\overline{w}_2-\overline{w}_1-\mu_2^2\frac{\partial^2\overline{w}_2}{\partial\xi_2^2}\right)\mathrm{d}\xi_1}}$$
$$+\overline{K}_t\left(\overline{w}_2-\mu_2^2\frac{\partial^2\overline{w}_2}{\partial\xi_2^2}\right)-\overline{K}_r\left(\frac{\partial^2\overline{w}_2}{\partial\xi_2^2}-\mu_2^2\frac{\partial^4\overline{w}_2}{\partial\xi_2^4}\right)=0, \tag{14b}$$

where

$$\chi=\frac{l_{b_2}}{l_{b_1}},\ \varrho_1^2=\frac{\rho_{b_2}A_{b_2}}{\rho_{b_1}A_{b_1}},\ \varrho_2^2=\frac{\rho_{b_2}I_{b_2}}{\rho_{b_1}I_{b_1}},\ \varrho_3^2=\frac{E_{b_2}I_{b_2}}{E_{b_1}I_{b_1}},$$
$$\overline{C}_{vdW}=\frac{C_{vdW}l_{b_1}^5}{E_{b_1}I_{b_1}},\ \overline{K}_t=\frac{K_tl_{b_1}^4}{E_{b_1}I_{b_1}},\ \overline{K}_r=\frac{K_rl_{b_1}^2}{E_{b_1}I_{b_1}}. \tag{15}$$

Due to the appearance of the coupling terms in Eqs. (14a) and (14b) (which are specified by the double-underlines), seeking an analytical solution to these integro-partial differential equations is not an easy task. In the following section, an efficient numerical scheme is proposed to find free dynamic response of the nanosystem.

3.2. Application of Galerkin approach to free vibration analysis of DOSWCNTs

Let premultiply both sides of Eqs. (14a) and (14b) by $\delta\overline{w}_1$ and $\delta\overline{w}_2$, respectively, then integrate the resulted statements over the dimensionless spatial domains of the nanotubes, and finally, add up the resulting expressions. After successful integration by parts, one can arrive at:

$$\int_{\xi_1=0}^{1}\left\{\left(\delta\overline{w}_1-\mu_1^2\frac{\partial^2\delta\overline{w}_1}{\partial\xi_1^2}\right)\frac{\partial^2\overline{w}_1}{\partial\tau^2}+\lambda_1^{-2}\left(\frac{\partial\delta\overline{w}_1}{\partial\xi_1}\frac{\partial^3\overline{w}_1}{\partial\tau^2\partial\xi_1}+\mu_1^2\frac{\partial^2\delta\overline{w}_1}{\partial\xi_1^2}\frac{\partial^4\overline{w}_1}{\partial\tau^2\partial\xi_1^2}\right)\right.$$
$$+\int_{\xi_2=0}^{\chi}\overline{C}_{vdW}\left(\delta\overline{w}_1-\mu_1^2\frac{\partial^2\delta\overline{w}_1}{\partial\xi_1^2}\right)\overline{w}_1\mathrm{d}\xi_2-\int_{\xi_2=0}^{\chi}\overline{C}_{vdW}\delta\overline{w}_1\overline{w}_2\mathrm{d}\xi_2+\frac{\partial^2\delta\overline{w}_1}{\partial\xi_1^2}\frac{\partial^2\overline{w}_1}{\partial\xi_2^2}$$
$$\left.+\overline{K}_t\left(\delta\overline{w}_1-\mu_1^2\frac{\partial^2\delta\overline{w}_1}{\partial\xi_1^2}\right)\overline{w}_1+\overline{K}_r\left(\frac{\partial\delta\overline{w}_1}{\partial\xi_1}\frac{\partial\overline{w}_1}{\partial\xi_1}+\mu_1^2\frac{\partial\delta\overline{w}_1}{\partial\xi_1^2}\frac{\partial^2\overline{w}_1}{\partial\xi_1^2}\right)\right\}\mathrm{d}\xi_1$$
$$+\int_{\xi_2=0}^{\chi}\left\{\varrho_1^2\left(\delta\overline{w}_2-\mu_2^2\frac{\partial^2\delta\overline{w}_2}{\partial\xi_2^2}\right)\frac{\partial^2\overline{w}_2}{\partial\tau^2}+\lambda_1^{-2}\varrho_2^2\left(\frac{\partial\delta\overline{w}_2}{\partial\xi_2}\frac{\partial^3\overline{w}_2}{\partial\tau^2\partial\xi_2}+\mu_2^2\frac{\partial^2\delta\overline{w}_2}{\partial\xi_2^2}\frac{\partial^4\overline{w}_2}{\partial\tau^2\partial\xi_2^2}\right)\right.$$
$$+\int_{\xi_1=0}^{1}\overline{C}_{vdW}\left(\delta\overline{w}_2-\mu_2^2\frac{\partial^2\delta\overline{w}_2}{\partial\xi_2^2}\right)\overline{w}_2\mathrm{d}\xi_1-\int_{\xi_1=0}^{1}\overline{C}_{vdW}\delta\overline{w}_2\overline{w}_1\mathrm{d}\xi_1+\varrho_3^2\frac{\partial^2\delta\overline{w}_2}{\partial\xi_2^2}\frac{\partial^2\overline{w}_2}{\partial\xi_2^2}$$
$$\left.+\overline{K}_t\left(\delta\overline{w}_2-\mu_2^2\frac{\partial^2\delta\overline{w}_2}{\partial\xi_2^2}\right)\overline{w}_2+\overline{K}_r\left(\frac{\partial\delta\overline{w}_2}{\partial\xi_2}\frac{\partial\overline{w}_2}{\partial\xi_2}+\mu_2^2\frac{\partial\delta\overline{w}_2}{\partial\xi_2^2}\frac{\partial^2\overline{w}_2}{\partial\xi_2^2}\right)\right\}\mathrm{d}\xi_2=0. \tag{16}$$

Using assumed mode method or modal analysis, the unknown fields of the suggested model are discretized in the spatial domain in terms of the mode shapes as: $\overline{w}_1(\xi_1,\tau)=\sum_{I=1}^{NM_1}\phi_I^{w_1}(\xi_1)\overline{w}_{1_I}(\tau)$ and $\overline{w}_2(\xi_2,\tau)=\sum_{I=1}^{NM_2}\phi_I^{w_2}(\xi_2)\overline{w}_{2_I}(\tau)$ where $NM_i,\phi_I^{w_i}$, and $\overline{w}_{i_I}$ in order are the number of vibration modes, Ith mode shape function, and the time-dependent parameters pertinent to the Ith mode of the ith tube. By substituting these statements into Eq. (16), the following set of second-order ordinary differential equations is obtained:

$$\begin{bmatrix}[\overline{\mathbf{M}}_b]^{w_1w_1} & [\overline{\mathbf{M}}_b]^{w_1w_2}\\ [\overline{\mathbf{M}}_b]^{w_2w_1} & [\overline{\mathbf{M}}_b]^{w_2w_2}\end{bmatrix}\begin{Bmatrix}\frac{\partial^2\overline{\mathbf{w}}_1}{\partial\tau^2}\\ \frac{\partial^2\overline{\mathbf{w}}_2}{\partial\tau^2}\end{Bmatrix}+\begin{bmatrix}[\overline{\mathbf{K}}_b]^{w_1w_1} & [\overline{\mathbf{K}}_b]^{w_1w_2}\\ [\overline{\mathbf{K}}_b]^{w_2w_1} & [\overline{\mathbf{K}}_b]^{w_2w_2}\end{bmatrix}\begin{Bmatrix}\overline{\mathbf{w}}_1\\ \overline{\mathbf{w}}_2\end{Bmatrix}=\begin{Bmatrix}\mathbf{0}\\ \mathbf{0}\end{Bmatrix}, \tag{17}$$

where

$$[\overline{\mathbf{M}}_\mathbf{b}]_{\mathbf{IJ}}^{\mathbf{w_1w_1}}=\int_0^1\left(\phi_\mathbf{I}^{\mathbf{w_1}}\phi_\mathbf{J}^{\mathbf{w_1}}+\lambda_1^{-2}\frac{\mathbf{d}\phi_\mathbf{I}^{\mathbf{w_1}}}{\mathbf{d}\xi_1}\frac{\mathbf{d}\phi_\mathbf{J}^{\mathbf{w_1}}}{\mathbf{d}\xi_1}-\mu_1^2\frac{\mathbf{d}^2\phi_\mathbf{I}^{\mathbf{w_1}}}{\mathbf{d}\xi_1^2}\left(\phi_\mathbf{J}^{\mathbf{w_1}}-\lambda_1^{-2}\frac{\mathbf{d}^2\phi_\mathbf{J}^{\mathbf{w_1}}}{\mathbf{d}\xi_1^2}\right)\right)\mathbf{d}\xi_1, \tag{18a}$$

$$[\overline{\mathbf{M}}_\mathbf{b}]_{\mathbf{IJ}}^{\mathbf{w_2w_2}}=\int_0^\chi\left(\varrho_1^2\phi_\mathbf{I}^{\mathbf{w_2}}\phi_\mathbf{J}^{\mathbf{w_2}}+\varrho_2^2\lambda_1^{-2}\frac{\mathbf{d}\phi_\mathbf{I}^{\mathbf{w_2}}}{\mathbf{d}\xi_2}\frac{\mathbf{d}\phi_\mathbf{J}^{\mathbf{w_2}}}{\mathbf{d}\xi_2}-\mu_2^2\frac{\mathbf{d}^2\phi_\mathbf{I}^{\mathbf{w_2}}}{\mathbf{d}\xi_2^2}\left(\varrho_1^2\phi_\mathbf{J}^{\mathbf{w_2}}-\lambda_1^{-2}\varrho_2^2\frac{\mathbf{d}^2\phi_\mathbf{J}^{\mathbf{w_2}}}{\mathbf{d}\xi_2^2}\right)\right)\mathbf{d}\xi_2, \tag{18b}$$

$$[\overline{\mathbf{K}}_\mathbf{b}]_{\mathbf{IJ}}^{\mathbf{w_1w_1}}=\int_0^1\begin{pmatrix}\frac{\mathbf{d}^2\phi_I^{w_1}}{\mathbf{d}\xi_1^2}\frac{\mathbf{d}^2\phi_J^{w_1}}{\mathbf{d}\xi_1^2}+\int_{\xi_2=0}^{\chi}\overline{C}_{vdW}\left(\phi_I^{w_1}-\mu_1^2\frac{\mathbf{d}^2\phi_I^{w_1}}{\mathbf{d}\xi_1^2}\right)\phi_J^{w_1}\mathbf{d}\xi_2+\\ \overline{K}_t\left(\phi_I^{w_1}-\mu_1^2\frac{\mathbf{d}^2\phi_I^{w_1}}{\mathbf{d}\xi_1^2}\right)\phi_J^{w_1}+\overline{K}_r\left(\frac{\mathbf{d}\phi_I^{w_1}}{\mathbf{d}\xi_1}-\mu_1^2\frac{\mathbf{d}^3\phi_I^{w_1}}{\mathbf{d}\xi_1^3}\right)\frac{\mathbf{d}\phi_J^{w_1}}{\mathbf{d}\xi_1}\end{pmatrix}\mathbf{d}\xi_1, \tag{18c}$$

$$[\overline{\mathbf{K}}_\mathbf{b}]_{\mathbf{IJ}}^{\mathbf{w_2w_2}}=\int_0^\chi\begin{pmatrix}\varrho_3^2\frac{\mathbf{d}^2\phi_I^{w_2}}{\mathbf{d}\xi_2^2}\frac{\mathbf{d}^2\phi_J^{w_2}}{\mathbf{d}\xi_2^2}+\int_{\xi_1=0}^{1}\overline{C}_{vdW}\left(\phi_I^{w_2}-\mu_2^2\frac{\mathbf{d}^2\phi_I^{w_2}}{\mathbf{d}\xi_2^2}\right)\phi_J^{w_2}\mathbf{d}\xi_1+\\ \overline{K}_t\left(\phi_I^{w_2}-\mu_2^2\frac{\mathbf{d}^2\phi_I^{w_2}}{\mathbf{d}\xi_2^2}\right)\phi_J^{w_2}+\overline{K}_r\left(\frac{\mathbf{d}\phi_I^{w_2}}{\mathbf{d}\xi_2}-\mu_2^2\frac{\mathbf{d}^3\phi_I^{w_2}}{\mathbf{d}\xi_2^3}\right)\frac{\mathbf{d}\phi_J^{w_2}}{\mathbf{d}\xi_2}\end{pmatrix}\mathbf{d}\xi_2, \tag{18d}$$

$$[\overline{\mathbf{K}}_\mathbf{b}]_{\mathbf{IJ}}^{\mathbf{w_1w_2}}=-\int_0^1\int_0^\chi\overline{\mathbf{C}}_{\mathbf{vdW}}\phi_\mathbf{I}^{\mathbf{w_1}}\phi_\mathbf{J}^{\mathbf{w_2}}\mathbf{d}\xi_1\mathbf{d}\xi_2, \tag{18e}$$

$$[\overline{\mathbf{K}}_\mathbf{b}]_{\mathbf{IJ}}^{\mathbf{w_2w_1}}=-\int_0^1\int_0^\chi\overline{\mathbf{C}}_{\mathbf{vdW}}\phi_\mathbf{I}^{\mathbf{w_2}}\phi_\mathbf{J}^{\mathbf{w_1}}\mathbf{d}\xi_1\mathbf{d}\xi_2. \tag{18f}$$

For evaluating the flexural frequencies of the nanosystem, the time-dependent parameters are assumed to be harmonic: $\overline{\mathbf{w}}_i(\tau)=\overline{\mathbf{w}}_{i_0}e^{i\varpi\tau};\ i=1,2$ where $\overline{\mathbf{w}}_{i_0}$ is the amplitude vectors of the ith tube, and ϖ represents the dimensionless flexural frequency. By introducing such a new version of $\overline{\mathbf{w}}_i$ to Eq. (17), and by solving the resulting set of eigenvalue equations for ϖ, the eigenvalues (i.e., dimensionless frequencies) and the pertinent eigenvectors (i.e., vibration modes) of the DOSWCNTs embedded in an elastic matrix are easily calculated.

4. Results and discussion

Consider a DOSWCNTs with the following data: $E_{b_i}=1$ TPa, $\nu_i=0.2$, $\rho_{b_i}=2300$ kg/m^3, $l_{b_i}=30$ nm, $r_{m_i}=1.5$ nm, $t_b=0.34$ nm, $d=r_{m_1}+r_{m_2}+2t_b$. Free transverse vibration of the nanosystem is studied under four boundary conditions, namely fully simply supported ends, fully clamped ends, simple-clamped ends, and clamped-free ends. These end conditions are, respectively, denoted by SS, CC, SC, and CF, and identically applied to both nanotubes. In the Galerkin approach, the mode shapes correspond to these boundary conditions should at least satisfy the geometrical conditions. For all numerical analysis, $NM_1=NM_2=13$. In view of this fact, the mode shapes pertinent to the above-mentioned boundary conditions for thin beams can be used as given in Refs. [76,77]. In the following parts, the influences of the crucial factors on the natural frequencies of such a system are going to be investigated.

4.1. Influence of the slenderness ratio

The effect of the slenderness ratio on the first five natural frequencies of the DOSWCNTs with different boundary conditions is of interest. In the case of a system of DOSWCNTs which is free from its surrounding elastic matrix, the obtained results have been demonstrated in Fig. 4 for three levels of the small-scale parameter (i.e., e_0a = 0, 1, and 2 nm). In all boundary conditions, by an increase of the slenderness ratio, the natural frequencies would reduce. For higher levels of the slenderness ratio, the influence of the slenderness ratio on the natural frequencies decreases. Additionally, the variation of the slenderness ratio is more influential on the frequencies of higher vibration modes. The fundamental frequencies of the nanosystem with SC and CF boundary conditions would increase as the small-scale parameter increases. In the cases of SS and CC end conditions, such frequencies would decrease with the small-scale parameter. The frequencies of higher-order modes of the nanostructure would generally decrease as the small-scale parameter magnifies. According to the plotted results in Fig. 4, the influence of the small-scale parameter on the natural frequencies of the nanosystem with lower slenderness ratio is more obvious.

4.2. Influence of the aspect ratio

An interesting study is carried out to determine the role of the aspect ratio (i.e., $\frac{l_{b2}}{l_{b1}}$) of DOSWCNTs on the natural frequencies. In Fig. 5, the first five frequencies of the nanosystem with $\lambda_1 = 30$ as a function of the aspect ratio are provided for various boundary conditions and three levels of the small-scale parameter. For all boundary conditions, the fundamental flexural frequency reduces by an increase of the aspect ratio. The effect of the aspect ratio on the fundamental frequency of the nanosystem increases as one moves from SS to CF, then SC, and finally CC boundary condition. For all end conditions, the effect of the aspect ratio on the second frequency is less obvious with respect to the fundamental one. In the cases of the CC and CF boundary conditions, variation of the aspect ratio has a trivial effect on the variation of the second fre-

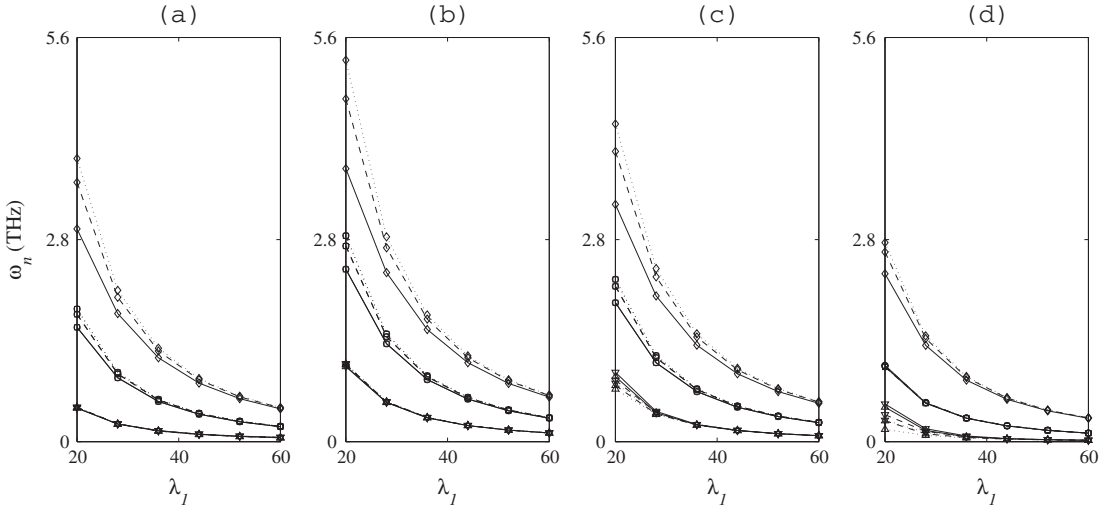

Fig. 4. Effect of the slenderness ratio on the first five natural frequencies of DOSWCNTs: (a) SS, (b) CC, (c) SC, (d) CF; ((. . .) e_0a = 0, (- - -) e_0a = 1, (—) e_0a = 2 nm; (△) ω_1, (▽) ω_2, (□) ω_3, (○) ω_4, (◇) ω_5; $K_t = K_r = 0$).

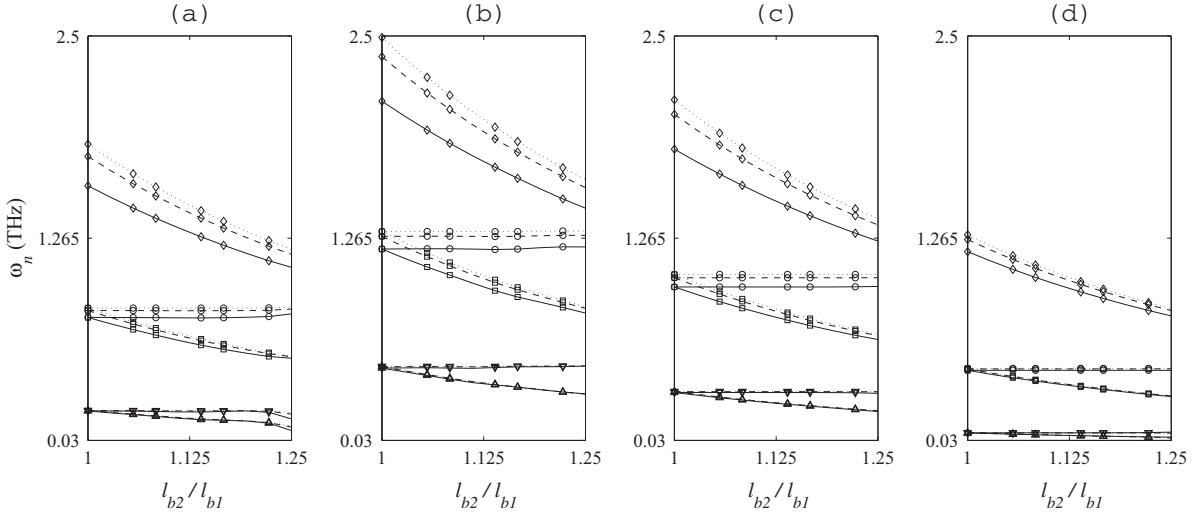

Fig. 5. Effect of the aspect ratio of DOSWCNTs on the first five natural frequencies of DOSWCNTs: (a) SS, (b) CC, (c) SC, (d) CF; ((. . .) $e_0a = 0$, (- - -) $e_0a = 1$, (—) e_0a = 2 nm; (△) ω_1, (▽) ω_2, (□) ω_3, (○) ω_4, (◇) ω_5; $\lambda_1 = 30$, $K_t = K_r = 0$).

quency. The third natural frequency of the DOSWCNTs would decrease as the aspect ratio increases. The rate of reduction is almost the same for all boundary conditions. Irrespective of the considered end conditions, the depicted results also display that the fourth frequency of the nanosystem slightly magnifies as the aspect ratio increases. The fifth frequency of the nanosystem would decrease as the aspect ratio increases. Such a reduction is roughly very similar for all considered end conditions. A close survey of the demonstrated results in Fig. 5 displays that the variation of the aspect ratio has the most influence on the variation of the fundamental frequency with respect to other frequencies. This fact holds true for all given boundary conditions. Generally, for a given aspect ratio, the predicted frequency of the nanosystem would decrease as the small-scale parameter magnifies.

4.3. Influence of the intertube distance

Another crucial parametric study is performed to investigate the effect of the intertube distance on the free vibration of DOSWCNTs systems. To this end, the predicted first five flexural frequencies of the nanosystem in terms of the free distance ratio of tubes (i.e., $\frac{d_0}{t_b} = \frac{d-(r_{m_1}+r_{m_2}+t_b)}{t_b}$) have been depicted in Fig. 6. The results are plotted for three levels of the small-scale parameter (i.e., e_0a = 0, 1, and 2 nm) and four boundary conditions in the case of $\lambda_1 = 25$. Irrespective of the considered boundary conditions, the natural frequency of the system of DOSWCNTs commonly decreases as the intertube distance increases. This is mainly related to this fact that by an increase of the intertube distance, the influence of the vdW force of each tube on another one would decrease. In other words, the interactional effects of the nanotubes or the share of the transverse stiffness of the vdW force density in the flexural stiffness of each tube would lessen. Concerning the first vibration mode, the effect of the intertube distance on the fundamental frequency of the nanosystem with a higher small-scale parameter is more apparent. In the cases of the nanosystem with SC and CF boundary conditions, the influence of the intertube distance on the second natural frequencies is so obvious with respect to other cases. In the case of CF boundary condition, the intertube distance on the fourth flexural frequency of the nanosystem is more influential. Additionally, variation of the intertube distance

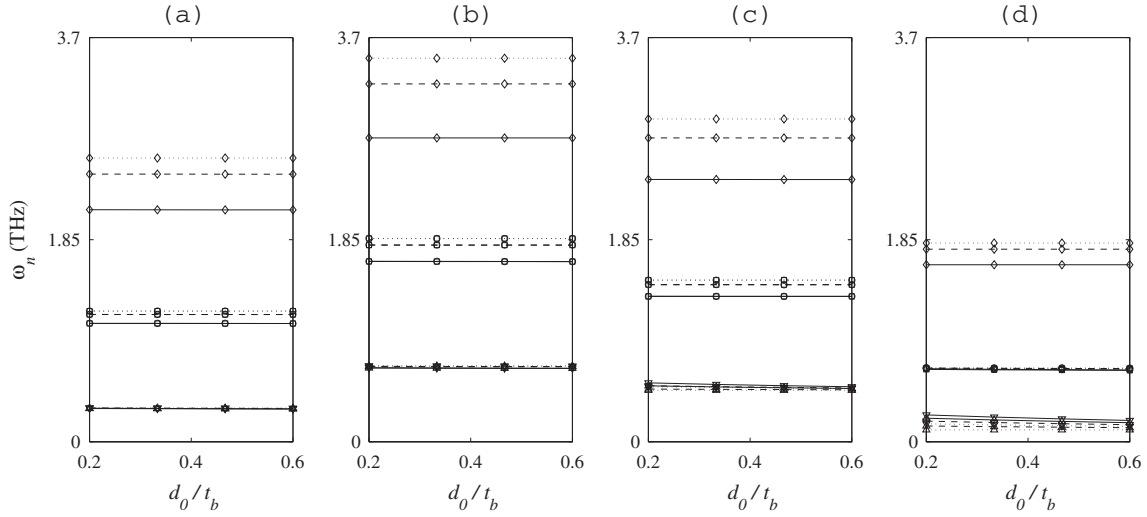

Fig. 6. Effect of the intertube distance on the first five natural frequencies of DOSWCNTs: (a) SS, (b) CC, (c) SC, (d) CF; ((. . .) $e_0a = 0$, (- - -) $e_0a = 1$, (—) e_0a = 2 nm; (△) ω_1, (▽) ω_2, (□) ω_3, (○) ω_4, (◇) ω_5; $\lambda_1 = 25$, $K_t = K_r = 0$).

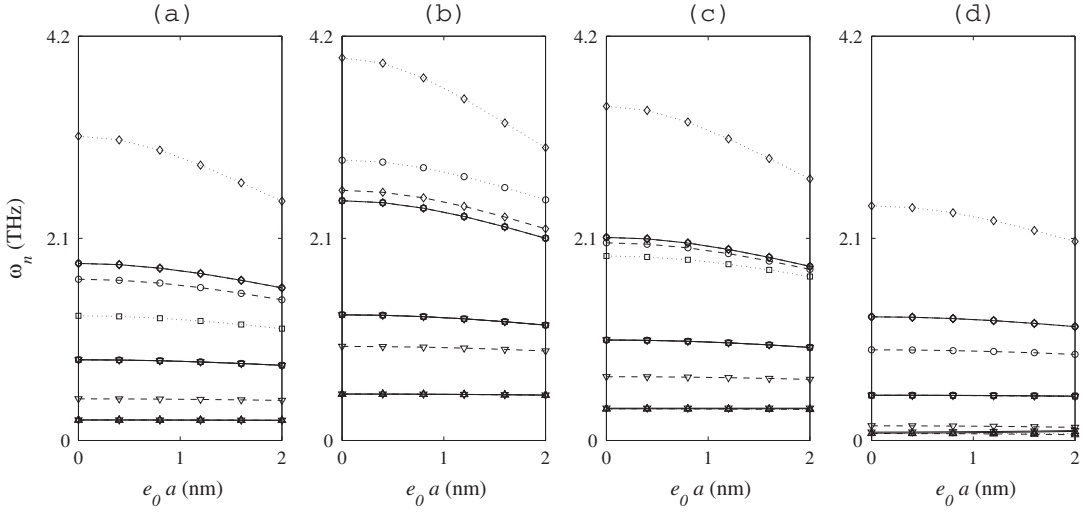

Fig. 7. Effect of the small-scale parameter on the first five natural frequencies of DOSWCNTs: (a) SS, (b) CC, (c) SC, (d) CF; ((. . .) $\frac{l_{b_2}}{l_{b_1}} = 0.4$, (- - -) $\frac{l_{b_2}}{l_{b_1}} = 0.7$, (—) $\frac{l_{b_2}}{l_{b_1}} = 1$; (△) ω_1, (▽) ω_2, (□) ω_3, (○) ω_4, (◇) ω_5; $\lambda_1 = 30$, $K_t = K_r = 0$).

has a trivial effect on the variation of the third frequency of the DOSWCNTs with SS, CC, and SC boundary conditions. Nevertheless, the third frequency of the nanosystem with CF condition would slightly decrease by an increase of the intertube distance.

4.4. Influence of the small-scale parameter

Equally important is to scrutiny the role of the small-scale parameter on the free dynamic response of the nanostructure. In Fig. 7, the predicted first five flexural frequencies of the DOSWCNTs with various boundary conditions have been plotted. The depicted results are provided for four boundary conditions with three levels of the aspect ratio (i.e., $\frac{l_{b_2}}{l_{b_1}} = 0.4$, 0.7, and 1), and $\lambda_1 = 30$. As it is seen, the fundamental frequency as well as the second frequency of the DOSWCNTs would slightly decrease as the small-scale parameter increases. The depicted results show that the influence of the aspect ratio on the vibration behavior of the nanosystem is also mode dependent. For instance, for all considered boundary conditions and small-scale parameters, the second frequency would reduce as the aspect ratio increases up to 1. However, the fundamental frequency of the nanosystem with CC end conditions commonly magnify with the aspect ratio. Additionally, the plotted results explain that the effect of the aspect ratio on the natural frequencies also relies to the boundary conditions of the nanosystem. For example, in the cases of CC and SC boundary conditions, the fundamental frequency magnifies as the aspect ratio increases, however, the fundamental frequencies of DOSWCNTs with SS and CF end conditions do not regularly vary in terms of the aspect ratio. Generally, the flexural frequencies of higher vibration modes are more influenced by the variation of the small-scale parameter as well as the aspect ratio. The plotted results in Fig. 7 show that the trends of the graphs of natural frequencies in terms of the small-scale parameter are not only affected by the aspect ratio but also by the mode number.

4.5. Influence of the surrounding elastic medium

A crucial study has been carried out to investigate the roles of the translational and rotational interactions of the nanosystem with its surrounding elastic environment. In Figs. 8 and 9, the first five frequencies of the elastically embedded DOSWCNTs as a function of transverse and rotational stiffness of the elastic matrix have

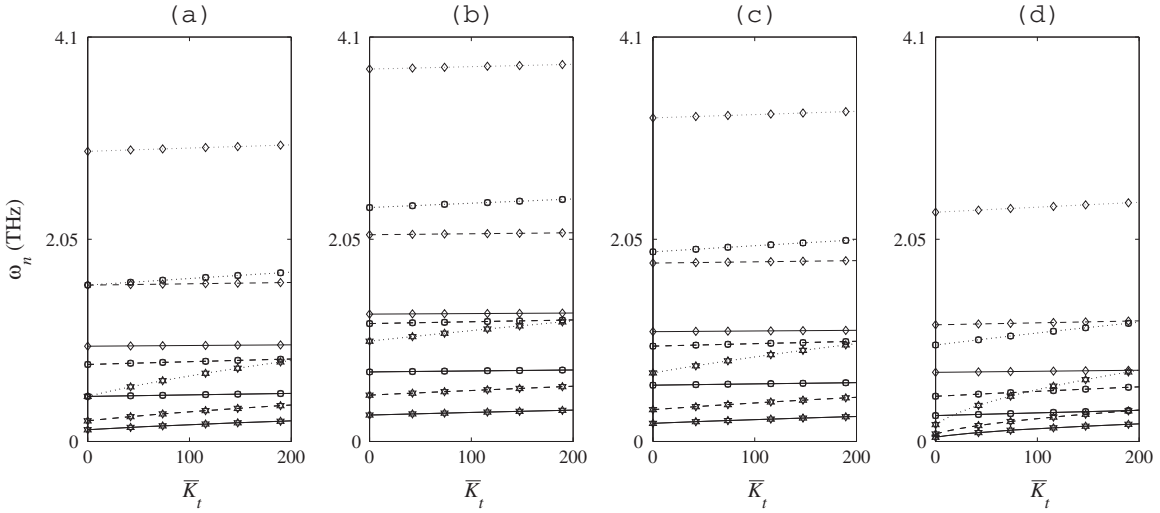

Fig. 8. Effect of the transverse stiffness of the surrounding environment on the first five natural frequencies of DOSWCNTs: (a) SS, (b) CC, (c) SC, (d) CF; ((. . .) $\lambda_1 = 20$, (---) $\lambda_1 = 30$, (—) $\lambda_1 = 40$; (△) ω_1, (▽) ω_2, (□) ω_3, (○) ω_4, (◇) ω_5; $e_0a = 2$ nm, $K_t = K_r = 0$).

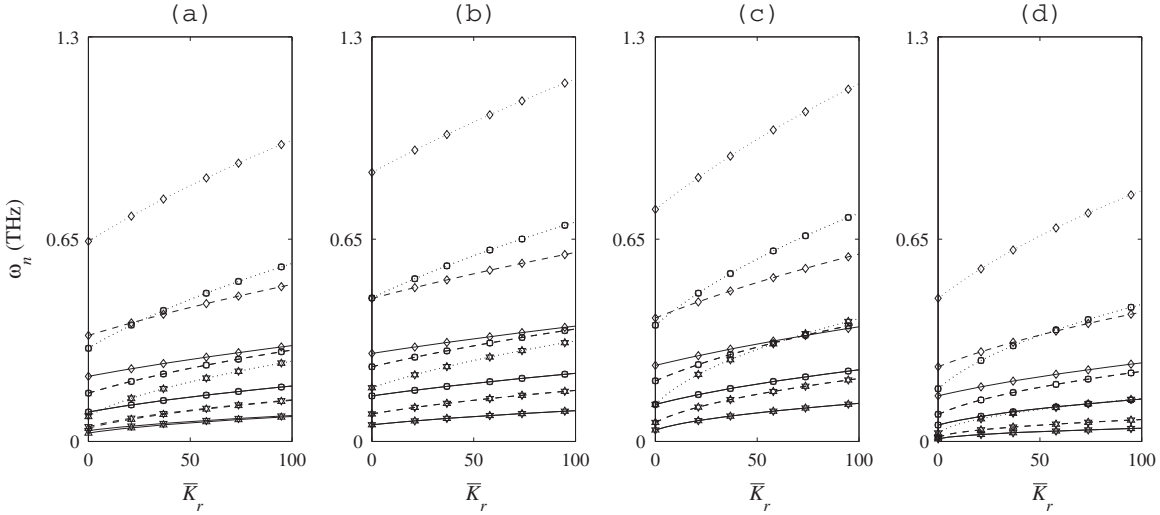

Fig. 9. Effect of the rotational stiffness of the surrounding environment on the first five natural frequencies of DOSWCNTs: (a) SS, (b) CC, (c) SC, (d) CF; ((. . .) $\lambda_1 = 20$, (---) $\lambda_1 = 30$, (—) $\lambda_1 = 40$; (△) ω_1, (▽) ω_2, (□) ω_3, (○) ω_4, (◇) ω_5; $e_0a = 2$ nm, $K_t = K_r = 0$).

been demonstrated, respectively. The plotted results are given for DOSWCNTs with tubes of identical length whose slenderness ratios are 20, 30, and 40. By an increase of both transverse and rotational stiffness of the surrounding elastic medium, the flexural frequencies of the nanosystem generally magnify. The frequencies of stockier DOSWCNTs (i.e., those with lower levels of slenderness ratio) are more influenced by the transverse and rotational stiffness of the elastic matrix. As a general result, variation of the transverse stiffness of the surrounding elastic medium is more influential on the fundamental frequency of the elastically embedded DOSWCNTs with respect to the frequencies of higher modes of vibration. Such an issue does not hold true for the effect of the rotational stiffness. In fact, the flexural frequencies associated with the higher vibration modes are more influenced by the rotational stiffness. For lower levels of the transverse or rotational stiffness of the surrounding medium, the influence of the transverse or rotational stiffness on the flexural frequencies of the nanosystem is more obvious. In view of the demonstrated results in Fig. 8(a)–(d), the fundamental frequencies of fully clamped (simply supported) DOSWCNTs are more (less) affected by the transverse stiffness of the surrounding medium. Such a fact also holds true for the effect of the rotational stiffness of the surrounding elastic matrix on the natural frequencies of the nanosystem.

5. Conclusions

In an attempt for better realizing the free dynamic response of elastically embedded DOSWCNTs, a suitable mathematical model is developed. By introducing a novel concept of the vdW force density function, a more rational continuum-based theory is developed for evaluating such an important interactional force in these nanosystems. By employing the Rayleigh beam theory in the context of the nonlocal continuum theory of Eringen, the equations of motion associated with the transverse vibration of the nanosystem are obtained. It was displayed that such equations are coupled integro-partial differential equations, and a special treatment should be implemented to solve them. Using Galerkin approach, the nonlocal governing equations are spatially discretized and the flexural frequencies are evaluated. Through various parametric studies, the effects of the slenderness ratio, intertube distance, aspect ratio, small-scale parameter, transverse and rotational stiffness of the surrounding elastic matrix on the dominant frequencies of the nanosystem are examined and discussed in some detail.

The proposed model in this paper is hoped to open a new horizon for modeling of doubly orthogonal membranes of SWCNTs at the vicinity of each other. Application of more sophisticated beam models in dynamic analysis of DOSWCNTs or even doubly orthogonal membranes would be beneficial when the length to diameter of the used SWCNTs is lower than a particular value. Such complementary studies provide basic steps towards rational modeling of and understanding the vibration mechanisms of more and more complex nanosystems such as multi-orthogonal-membranes of SWCNTs. Surely, these advanced explorations lead to a better realization of the mechanics of jungles of CNTs which are going to be widely exploited in advanced technologies of MEMS and NEMS in the near future.

Acknowledgement

The financial support of the Iran National Science Foundation (INSF) as well as Iran Nanotechnology Initiative Council for the undertaken work is gratefully acknowledged.

References

[1] Sazonova V, Yaish Y, Üstünel H, Roundy D, Arias TA, McEuen PL. A tunable carbon nanotube electromechanical oscillator. Nature 2004;431:284–7.
[2] Yoon J, Ru CQ, Mioduchowski A. Timoshenko-beam effects on transverse wave propagation in carbon nanotubes. Compos Part B-Eng 2004;35:87–93.
[3] Li C, Chou TW. Single-walled carbon nanotubes as ultrahigh frequency nanomechanical resonators. Phys Rev B 2003;68:073405.
[4] Eklund PC, Holden JM, Jishi RA. Vibrational modes of carbon nanotubes; spectroscopy and theory. Carbon 1995;33:959–72.
[5] Huttel AK, Steele GA, Witkamp B, Poot M, Kouwenhoven LP, van der Zant HS. Carbon nanotubes as ultrahigh quality factor mechanical resonators. Nano Letters 2009;9:2547–52.
[6] Liu JZ, Zheng Q, Jiang Q. Effect of a rippling mode on resonances of carbon nanotubes. Phys Rev Lett 2001;86:4843.
[7] Gibson RF, Ayorinde EO, Wen YF. Vibrations of carbon nanotubes and their composites: a review. Compos Sci Technol 2007;67:1–28.
[8] Arash B, Wang Q. A review on the application of nonlocal elastic models in modeling of carbon nanotubes and graphenes. Comput Mater Sci 2012;51:303–13.
[9] Wang Q, Arash B. A review on applications of carbon nanotubes and graphenes as nano-resonator sensors. Comput Mater Sci 2014;82:350–60.
[10] Saito R, Dresselhaus G, Dresselhaus MS. Physical properties of carbon nanotubes, vol. 4. London: Imperial College Press; 1998.
[11] Treacy MMJ, Ebbesen TW, Gibson JM. Exceptionally high Young's modulus observed for individual carbon nanotubes. Nature 1996;381:678–80.
[12] Coleman JN, Khan U, Blau WJ, Gu'ko YK. Small but strong: a review of the mechanical properties of carbon nanotube-polymer composites. Carbon 2006;44:1624–52.
[13] Salvetat-Delmotte JP, Rubio A. Mechanical properties of carbon nanotubes: a fiber digest for beginners. Carbon 2002;40:1729–34.
[14] Yakobson BI, Avouris P. Mechanical properties of carbon nanotubes. In: Carbon nanotubes. Berlin Heidelberg: Springer; 2001. p. 287–327.
[15] Kong J, Chapline MG, Dai H. Functionalized carbon nanotubes for molecular hydrogen sensors. Adv Mater 2001;13:1384.
[16] Tung S, Rokadia H, Li WJ. A micro shear stress sensor based on laterally aligned carbon nanotubes. Sensor Actuat A-Phys 2007;133:431–8.
[17] Souayeh S, Kacem N. Computational models for large amplitude nonlinear vibrations of electrostatically actuated carbon nanotube-based mass sensors. Sensor Actuat A-Phys 2014;208:10–20.
[18] Li C, Chou TW. Mass detection using carbon nanotube-based nanomechanical resonators. Appl Phys Lett 2004;84:5246–8.
[19] Witkamp B, Poot M, van der Zant HS. Bending-mode vibration of a suspended nanotube resonator. Nano Letters 2006;6:2904–8.
[20] Mei J, Li L. Frequency self-tuning of carbon nanotube resonator with application in mass sensors. Sensor Actuat B-Chem 2013;188:661–8.
[21] Majumder M, Chopra N, Andrews R, Hinds BJ. Nanoscale hydrodynamics: enhanced flow in carbon nanotubes. Nature 2005;438:44.
[22] Ko GH, Heo K, Lee K, Kim DS, Kim C, Sohn Y, et al. An experimental study on the pressure drop of nanofluids containing carbon nanotubes in a horizontal tube. INT J Heat Mass Transfer 2007;50:4749–53.
[23] Joseph S, Aluru NR. Why are carbon nanotubes fast transporters of water? Nano Letters 2008;8:452–8.
[24] Bianco A, Kostarelos K, Prato M. Applications of carbon nanotubes in drug delivery. Curr Opin Chem Biol 2005;9:674–9.
[25] Prakash S, Kulamarva AG. Recent advances in drug delivery: potential and limitations of carbon nanotubes. Recent Pat Drug Deliv Formul 2007;1:214–21.
[26] Liu Z, Robinson JT, Tabakman SM, Yang K, Dai H. Carbon materials for drug delivery and cancer therapy. Mater Today 2011;14:316–23.
[27] Madani SY, Naderi N, Dissanayake O, Tan A, Seifalian AM. A new era of cancer treatment: carbon nanotubes as drug delivery tools. Int J Nanomed 2011;6:2963.
[28] Dequesnes M, Rotkin SV, Aluru NR. Calculation of pull-in voltages for carbon-nanotube-based nanoelectromechanical switches. Nanotechnology 2002;13:120.
[29] Sapmaz S, Blanter YM, Gurevich L, Van der Zant HSJ. Carbon nanotubes as nanoelectromechanical systems. Phys Rev B 2003;67:235414.
[30] Jang JE, Cha SN, Choi Y, Amaratunga GAJ, Kang DJ, Hasko DG, et al. Nanoelectromechanical switches with vertically aligned carbon nanotubes. Appl Phys Lett 2005;87:163114.
[31] Hierold C, Jungen A, Stampfer C, Helbling T. Nano electromechanical sensors based on carbon nanotubes. Sensor Actuat A-Phys 2007;136:51–61.
[32] Hsu JC, Chang RP, Chang WJ. Resonance frequency of chiral single-walled carbon nanotubes using Timoshenko beam theory. Phys Lett A 2008;372:2757–9.
[33] Kiani K. Longitudinal, transverse, and torsional vibrations and stabilities of axially moving single-walled carbon nanotubes. Curr Appl Phys 2013;13:1651–60.
[34] Kiani K. A meshless approach for free transverse vibration of embedded single-walled nanotubes with arbitrary boundary conditions accounting for nonlocal effect. Int J Mech Sci 2010;52:1343–56.

[35] Simsek M. Nonlocal effects in the forced vibration of an elastically connected double-carbon nanotube system under a moving nanoparticle. Comput Mater Sci 2011;50:2112–23.
[36] Kiani K, Wang Q. On the interaction of a single-walled carbon nanotube with a moving nanoparticle using nonlocal Rayleigh, Timoshenko, and higher-order beam theories. Eur J Mech A-Solid 2012;31:179–202.
[37] Kiani K. Nonlinear vibrations of a single-walled carbon nanotube for delivering of nanoparticles. Nonlinear Dyn 2014;76:1885–903.
[38] Wang Q. Wave propagation in carbon nanotubes via nonlocal continuum mechanics. J Appl Phys 2005;98:124301.
[39] Wang L, Hu H. Flexural wave propagation in single-walled carbon nanotubes. Phys Rev B 2005;71:195412.
[40] Hu YG, Liew KM, Wang Q, He XQ, Yakobson BI. Nonlocal shell model for elastic wave propagation in single-and double-walled carbon nanotubes. J Mech Phys Solids 2008;56:3475–85.
[41] Heireche H, Tounsi A, Benzair A, Maachou M, Adda Bedia EA. Sound wave propagation in single-walled carbon nanotubes using nonlocal elasticity. Physica E 2008;40:2791–9.
[42] Liew KM, Hu Y, He XQ. Flexural wave propagation in single-walled carbon nanotubes. J Comput Theor Nanosci 2008;5:581–6.
[43] Lee HL, Chang WJ. Free transverse vibration of the fluid-conveying single-walled carbon nanotube using nonlocal elastic theory. J Appl Phys 2008;103:024302.
[44] Chang WJ, Lee HL. Free vibration of a single-walled carbon nanotube containing a fluid flow using the Timoshenko beam model. Phys Lett A 2009;373:982–5.
[45] Zhen Y, Fang B. Thermal-mechanical and nonlocal elastic vibration of single-walled carbon nanotubes conveying fluid. Comput Mater Sci 2010;49:276–82.
[46] Kiani K. Nanofluidic flow-induced longitudinal and transverse vibrations of inclined stocky single-walled carbon nanotubes. Comput Method Appl Mech Eng 2014;276:691–723.
[47] Yang J, Ke LL, Kitipornchai S. Nonlinear free vibration of single-walled carbon nanotubes using nonlocal Timoshenko beam theory. Physica E 2010;42:1727–35.
[48] Farshidianfar A, Soltani P. Nonlinear flow-induced vibration of a SWCNT with a geometrical imperfection. Comput Mater Sci 2012;53:105–16.
[49] Kiani K. Nanoparticle delivery via stocky single-walled carbon nanotubes: a nonlinear-nonlocal continuum-based scrutiny. Compos Struct 2014;116:254–72.
[50] Murmu T, Adhikari S. Nonlocal transverse vibration of double-nanobeam-systems. J Appl Phys 2010;108:083514.
[51] Murmu T, Adhikari S. Nonlocal elasticity based vibration of initially pre-stressed coupled nanobeam systems. Eur J Mech A-Solid 2012;34:52–62.
[52] Kiani K. Nonlocal continuous models for forced vibration analysis of two- and three-dimensional ensembles of single-walled carbon nanotubes. Physica E 2014;60:229–45.
[53] Kiani K. In- and out-of- plane dynamic flexural behaviors of two-dimensional ensembles of vertically aligned single-walled carbon nanotubes. Physica B 2014;449:164–80.
[54] Kiani K. Nonlocal discrete and continuous modeling of free vibration of stocky ensembles of single-walled carbon nanotubes. Curr Appl Phys 2014;14:1116–39.
[55] He LH, Lim CW, Wu BS. A continuum model for size-dependent deformation of elastic films of nano-scale thickness. Int J Solids Struct 2004;41:847–57.
[56] Alizada AN, Sofiyev AH. Modified Young's moduli of nano-materials taking into account the scale effects and vacancies. Meccanica 2011;46:915–20.
[57] Song F, Huang GL, Park HS, Liu XN. A continuum model for the mechanical behavior of nanowires including surface and surface-induced initial stresses. Int J Solids Struct 2011;48:2154–63.
[58] Wang BL, Wang KF. Vibration analysis of embedded nanotubes using nonlocal continuum theory. Compos Part B-Eng 2013;47:96–101.
[59] Benguediab S, Tounsi A, Zidour M, Semmah A. Chirality and scale effects on mechanical buckling properties of zigzag double-walled carbon nanotubes. Compos Part B-Eng 2014;57:21–4.
[60] Aifantis EC. On the microstructural origin of certain inelastic models. Trans ASME J Mater Eng Technol 1984;106:326–30.
[61] Triantafyllidis N, Aifantis EC. A gradient approach to localization of deformation-I. Hyperelastic materials. J Elasticity 1986;16:225–38.
[62] Askes H, Aifantis EC. Gradient elasticity and flexural wave dispersion in carbon nanotubes. Phys Rev B 2009;80:195412.
[63] Ansari R, Gholami R, Rouhi H. Vibration analysis of single-walled carbon nanotubes using different gradient elasticity theories. Compos Part B-Eng 2012;43:2985–9.
[64] Zheng Y, Zhang H, Chen Z, Ye H. Size and surface effects on the mechanical behavior of nanotubes in first gradient elasticity. Compos Part B-Eng 2012;43:27–32.
[65] Ghavanloo E, Fazelzadeh SA. Free vibration analysis of orthotropic doubly-curved shallow shells based on the gradient elasticity. Compos Part B-Eng 2013;45:1448–57.
[66] Daneshmand F. Combined strain-inertia gradient elasticity in free vibration shell analysis of single walled carbon nanotubes using shell theory. Appl Math Comput 2014;243:856–69.
[67] Zhang B, He Y, Liu D, Gan Z, Shen L. Non-classical Timoshenko beam element based on the strain gradient elasticity theory. Finite Elem Anal Des 2014;79:22–39.
[68] Eringen AC, Edelen DGB. On nonlocal elasticity. Int J Eng Sci 1972;10:233–48.
[69] Eringen AC. Linear theory of nonlocal elasticity and dispersion of plane waves. Int J Eng Sci 1972;10:425–35.
[70] Eringen AC. Nonlocal polar elastic continua. Int J Eng Sci 1972;10:1–16.
[71] Eringen AC. Nonlocal continuum field theories. New York: Springer-Verlag; 2002.
[72] Lennard-Jones JE. The determination of molecular fields: from the variation of the viscosity of a gas with temperature. Proc Royal Soc Lon Ser A 1924;106:441–62.
[73] Peddieson J, Buchanan GR, McNitt RP. Application of nonlocal continuum models to nanotechnology. Int J Eng Sci 2003;41:305–12.
[74] Wang Q, Liew KM. Application of nonlocal continuum mechanics to static analysis of micro- and nano-structures. Phys Lett A 2007;363:236–42.
[75] Duan WH, Wang CM, Zhang YY. Calibration of nonlocal scaling effect parameter for free vibration of carbon nanotubes by molecular dynamics. J Appl Phys 2007;101:024305.
[76] Reddy JN. Mechanics of laminated composite plates and shells: theory and analysis. CRC Press; 2004.
[77] Szilard R. Theories and applications of plate analysis: classical numerical and engineering methods. John Wiley and Sons; 2004.